UCSF
UC San Francisco Previously Published Works

Title
Water Is a Cagey Liquid

Permalink
https://escholarship.org/uc/item/58g6498m

Journal
Journal of the American Chemical Society, 140(49)

ISSN
0002-7863

Authors
Urbic, Tomaz
Dill, Ken A

Publication Date
2018-12-12

DOI
10.1021/jacs.8b08856

Peer reviewed

eScholarship.org Powered by the California Digital Library
University of California

Author Manuscript

Author Manuscript

Author Manuscript

Author Manuscript

HHS Public Access

Author manuscript

J Am Chem Soc. Author manuscript; available in PMC 2019 December 12.

Published in final edited form as:

J Am Chem Soc. 2018 December 12; 140(49): 17106–17113. doi:10.1021/jacs.8b08856.

Water Is a Cagey Liquid

Tomaz Urbic[*,†], **Ken A. Dill**[‡]

[†]Faculty of Chemistry and Chemical Technology, University of Ljubljana, Večna pot 113, Ljubljana SI-1000, Slovenia

[‡]Laufer Center for Physical and Quantitative Biology and Departments of Chemistry and of Physics & Astronomy, Stony Brook University, Stony Brook, New York 11794-5252, United States

Abstract

Liquid water is considered poorly understood. How are water's physical properties encoded in its molecular structure? We introduce a statistical mechanical model (CageWater) of water's hydrogen-bonding (HB) and Lennard−Jones (LJ) interactions. It predicts the energetic and volumetric and anomalous properties accurately. Yet, because the model is analytical, it is essentially instantaneous to compute. This model advances our understanding beyond current molecular simulations and experiments. Water has long been regarded as a "2-density liquid": a dense LJ liquid and a looser HB one. Instead, we find here a different antagonism underlying water structure−property relations: HBs in water−water pairs drive density, while HBs in cooperative cages drive openness. The balance shifts strongly with temperature and pressure. This model interprets the molecular structures underlying the liquid−liquid phase transition in supercooled water. It may have value in geophysics, biomolecular modeling, and engineering of materials for water purification and green chemistry.

Graphical Abstract

[*]Corresponding Author: tomaz.urbic@fkkt.uni-lj.si.

Supporting Information

The Supporting Information is available free of charge on the ACS Publications website at DOI: 10.1021/jacs.8b08856.

Details of the theory, water models used for comparison, additional results (PDF)

The authors declare no competing financial interest.

Author Manuscript Author Manuscript Author Manuscript Author Manuscript

INTRODUCTION

A goal of material science is to model how the properties of materials derive from their molecular structures. For liquid water, this has been difficult. Despite its importance and extensive studies, liquid water is considered “poorly understood”.[1] Water has anomalous properties (in its ambient and supercooled density, compressibility, expansion coefficient, and heat capacity vs temperature and pressure). It is difficult to model because of water’s strong cohesion and incommensurate forces. Like other molecules, water has radial repulsive and attractive forces. However, unlike most others, water molecules also engage in strong tetrahedral hydrogen bonding, which drives intermolecular heterogeneous cage-like clustering.

While computer simulations of explicit water models such as TIP, SPC, ST2, and mW[1–6] play an important role, simulations alone are not the “understanding” that is often sought. From simulations, the chain of logic from molecules to macroscopics can be corrupted by convergence and sampling errors, so such simulations are challenged to give derivative properties such as heat capacities, compressibilities and expansion coefficients, structural populations, free energies, and entropies and to sample weakly populated multibody heterogeneous structures such as networks and cages. Yet, the alternative—theoretical modeling[1,7–34]—rarely predicts properties with quantitative accuracy because of water’s complexity.

Author Manuscript Author Manuscript Author Manuscript Author Manuscript

Theories dating back to 1892[35] explain liquid water's anomalies as resulting from mixture of high-density and low-density components.[26,28,29,36–43] Yet, no molecular theory addresses these key questions: What are the structures and populations of those molecular assemblies? How does molecular organization change with temperature and pressure? Do the components ever become two distinct stable states, as has been postulated for the liquid −liquid transition of supercooled water?[7,26,28,29,36,41] Here, we develop a statistical mechanical theory of liquid water (CageWater) based on radial contacts, tetrahedral hydrogen bonding, and multiwater cages. It is analytical, so it computes properties essentially instantaneously as derivatives of a partition function, predicts experiments to within a few percent over the range of temperatures for which data is available, and gives interpretations of bulk properties in terms of the molecular physics.

THEORY

We model water molecules as spheres that can have radial contact interactions or tetrahedral hydrogen bonds with neighboring water molecules, Figure 1.[44–46] Two water molecules can interact through a hydrogen bond (which depends on their relative orientations), interact through a contact (which is orientation independent and occurs when they are close in space and no HB is present), or be noninteracting (when they are far apart, as in van der Waals gas). Hydrogen bonds are further parsed into two types: an HB can occur between 2 adjacent waters that have no higher order structure or can occur within a 12-water hexagonal unit cell (cage). The liquid state is assumed to have an underlying intrinsic hexagonal (ice Ih) lattice structure, from which the liquid is a perturbation. We focus on a test molecule that occupies one lattice site and its interaction with its clockwise next-neighbor.

i. In pairwise hydrogen bond (2HB) the test water molecule can point one of its four hydrogen-bonding arms at an angle θ to within $\pi/3$ of the center of its neighbor water, which is equivalent to about one-fourth of its full solid angle.[45,46] This water is considered to be H bonded to a neighboring water if each one has an arm that is colinear with the other. The HB strength is maximal if the arms are perfectly colinear and weakens as the angle between the arms increases according to

$$u_{\mathrm{HB}}(\theta) = -\epsilon_{\mathrm{HB}} + k_{\mathrm{s}}(1+\cos\theta)^2, 0 < \theta < \pi/3 \quad (1)$$

where ϵ_{HB} is an HB energy constant of the maximal HB strength and k_{s} is the angular spring constant. There are no donors or acceptors; the strength depends only on the angle of alignment.

ii. In pairwise contact (c) the test water forms a contact with its clockwise neighbor but no hydrogen bond. The energy of this state is

$$u_{\mathrm{c}}(\theta) = -\epsilon_{\mathrm{c}}, 0 < \theta < \pi/3 \quad (2)$$

independent of orientation when two molecules are in contact.

Author Manuscript Author Manuscript Author Manuscript Author Manuscript

iii. Pairwise noninteraction (0) occurs with energy $u_0(\theta) = 0$.

iv. A hydrogen-bonded cage (cage) is a water unit cell, which has 12 hydrogen bonds. We assume the same HB potential as above, except with a larger volume and an additional favorable cooperativity energy; see eq 3.

Now, for each of the 4 states—a 2-water HB (2HB), a cage HB (cage), a contact (c), or a noninteraction (0)—we construct a Boltzmann factor from the energy above and integrate over all angles ϕ, θ, and ψ and over all of the separations x, y, and z of the test molecule that satisfy the limits defined above to obtain, in each case, an isobaric− isothermal ensemble component partition function Δ_{2HB}, Δ_{cage}, Δ_c, or Δ_0; see SI A for details. We then sum them as follows into a total partition function, Δ, for the 12 test waters forming 15 hydrogen bonds

$$\Delta(T, p) = \left(\Delta_{2HB} + \Delta_c + \Delta_o\right)^{15} - \Delta_{2HB}^{15} + \delta\Delta_{cage}^{15} \quad (3)$$

where $\delta = \exp(-\beta\epsilon_{cor})$ is the Boltzmann factor for the cooperativity energy, ϵ_{cor}, that applies only when 12 water molecules form a full cage of 15 hydrogen bonds. The term $\Delta^{15}{}_{2HB}$ is subtracted here to avoid double counting of HBs that are in cages. On one hand, we are not aware of experimental evidence specifically showing 12-mer cages in liquid water. On the other hand, our 12-mers are just a convenient way to invoke a single term in an analytical model to capture experimentally known cage-like cooperativities beyond dimers. Moreover, the lack of experimental evidence is to be expected since a key conclusion that we will find here is the prediction that large thermodynamic consequences of cages arise from very small populations of them.

Now we combine the Boltzmann factors for the individual water molecules to get the partition function for the whole system of N particles; the population of different states can be calculated[44–46] as well as all of the other thermodynamic properties from simple derivations of the partition function as described previously.[44–48] The attraction beyond the pair level is treated in the mean field as an attractive energy,[49] $-Na/v$, among hexagons, where a is the van der Waals dispersion parameter[44,47,48] and v is the average molar volume. Parameters needed for calculations were obtained by getting good agreement with a temperature dependence of the density at normal pressure and of boiling point position and are presented in Table S1. Finally, all of the volumetric and energetic properties of liquid water in the model are calculated directly using standard statistical thermodynamics derivatives of the partition function.[50]

RESULTS AND DISCUSSION

Comparing the model to experiments and atomistic simulations. Here, we compare the measured properties over water's liquid range to those predicted by CageWater experiment and by best practices water simulation models: TIP4P/2005, TIP3P, SPC, and mW (see SI section B).

Author Manuscript Author Manuscript Author Manuscript Author Manuscript

Volumetric and Thermal Properties, Including Anomalies, of Liquid Water.

Temperature Dependences of the Volumetric Properties.—Figure 2 shows the temperature dependences over the normal liquid water range of the four main thermal and volumetric properties of water: the density, ρ, the thermal expansion coefficient, α, the isothermal compressibility, κ, and the heat capacity, C_p (Figure 2a). The black line shows the model predictions, the red triangles are the experimental data,[9] and the lines show published simulation results from TIP4P/2005,[4] TIP3P, and SPC water[5] and the mW model.[6] Compared to experiments, the present model gives equal or better agreement than the simulational models over the normal and supercooled liquid temperature range and does not have the fluctuation errors that simulations have.

The model allows us to parse the experimental observables into hydrogen-bonding, caging, van der Waals, and noninteracting molecular components. Water is known to have a high heat capacity (ability to absorb thermal energy upon heating) among liquids of similar molecular size. Here are the main conclusions from Figure 2b. (1) In the normal liquid range, the high heat capacity comes from the breaking of two types of bonds: pairwise H bonds and Lennard−Jones-like contacts. (2) Heating hot water near the boiling point leads to lower density, as it would for any LJ fluid, because heating hot water changes the contact interactions more than the H bonds.

Temperature Dependences of Hydrogen Bonding.—Additional experiments show how water's hydrogen bonding depends on temperature. Figure 3a compares the computed fraction of hydrogen bonds that are broken as a function of temperature with Raman experiments of Hare and Sorensen[51] in the OH stretch region of water (2900−3800 cm^{-1}). Figure 3b–d shows a related quantity, the average number of hydrogen bonds made per water molecule, vs temperature. Figure 3b shows the temperature dependence of the average number of H bonds per water molecule, n_{HB}. While the experiments and atomistic simulations have inevitable scatter, the CageWater model, because it is analytical, does not. n_{HB} at room temperature varies from 2 to 4. This scatter can be attributed to a number of factors, such as differences in the definition of the HB, limitations in experimental/simulation techniques, different experimental conditions, and ambiguities in the interpretation of experimental data.[52–60] Spectroscopic experiments require assigning spectral features to whether or not a hydrogen bond is formed. This can involve some arbitrary choices. Also, it can depend on whether a hydrogen bond is defined structurally or energetically. Figure 3c shows differences and a changing tendency of n_{HB} estimated from molecular simulations and spectrum studies. Nevertheless, irrespective of the details, n_{HB} generally decreases with increasing temperature.

Pressure Dependences of the Volumetric Properties.—Figure 2c shows the same bulk properties as in Figure 2a except now computed as a function of pressure, not temperature. As increasing pressure squeezes water to become more compact (density increases and compressibility decreases), it crumples the hexagonal water cages breaking them into component pieces that just have pairwise water−water hydrogen bonding with little change to LJ and noninteracting water populations. Pressure decreases the heat capacity (bond-breaking capability) because although it melts out some cages it is also

Author Manuscript Author Manuscript Author Manuscript Author Manuscript

"freezing in" some pairwise H bonds. The thermal expansion coefficient increases with pressure because pressure melts out the rigid cages into fragmented H-bond pairs, which can be more readily squeezed together by pressure.

Supercooled Water and the Putative Liquid-Liquid Phase Transition.

Here, we seek insights into the widely discussed issue of whether supercooled water undergoes a liquid−liquid phase transition. Model studies have explored how liquid−liquid phase behavior depends on the balance of LJ and H-bond interactions[25] as we also do here. In supercooling, water is prevented from freezing below its normal freezing point by carefully avoiding nucleation, presently to around −45 °C.[62] The central observation is that lowering the temperature to supercool water below its freezing point leads to a decreased density and thermal expansion coefficient (which is negative in that region) and to an increasing divergence of isothermal compressibility κ and isobaric heat capacity C_p (see Figure 2 for the data and atomistic simulations).[1,42,63] These divergences have been explained either as water reaching a spinodal point, beyond which there is no further metastable liquid phase and only the solid frozen phase, or a phase transition between two different metastable liquid phases.[1,64–68] Common to these two explanations is the existence of singularities associated with diverging density fluctuations at low temperatures. Sastry et al.[7,69] showed that the simplest interpretation of the behavior of supercooled water consistent with experimental observations is free of singularities. The two phases have been postulated to be a high-density liquid (HDL) and a low-density liquid (LDL).[64,71] Although Limmer and Chandler[66] explained this transition as crystallization, rather than as a liquid −liquid change, Palmer and co-workers[70,72] have shown decisively that the crystallization interpretation is an artifact of an error in the Monte Carlo codes of Limmer and Chandler. Hence, evidence is now quite clear that supercooling entails a liquid−liquid transition.

Getting definitive answers is challenging for experiments because of the difficulty in cooling supercooled water to even lower temperatures without freezing.[73] Also, it is challenging for molecular simulations because of the small model system sizes (typically a few hundred waters), the slow speeds, and poor convergence in determining state populations in these cold low-barrier phase equilibria.[43,74–83] In addition, of course, the water models used in simulations are only imperfect models of reality. Thus, in this controversy simulation models are called "water-like". In that same spirit, we regard CageWater too as water-like.

Nevertheless, the present model gives new insights here because (i) it samples state populations completely and with no sampling errors, so it allows for definitive conclusions about whether or not the model predicts a true thermodynamic phase transition and critical point, (ii) it is not limited by slow kinetics, (iii) in the normal liquid region, it fits the full pVT profiles as accurately as TIP4P/2005, which is regarded as the current best model for pure water, and (iv) it is not confounded by a freezing transition because CageWater only models the liquid state. Here are the model predictions.

First, Figure 4 shows that CageWater accurately reproduces the anomalous hallmark thermal and volumetric signatures of the LLPT, namely, the divergent increasing heat capacity and compressibility with lowered temperature. Moreover, this model gives the microscopic components of those observables. We find that the large diverging heat capacity is due to the

Author Manuscript Author Manuscript Author Manuscript Author Manuscript

water cages, which have dominant populations in cold and supercooled water. The heat capacity is the sum of two contributions for each state: the population of that state multiplied by the individual heat capacity. We also find that the negative thermal expansion of supercooled water is dominated by the cage term. Heating supercooled water shrinks the average volume by melting the cages, which are voluminous, and converts them to smaller H-bonded fragments, like breaking a glass jar into shards that pack more compactly. This same physics is reflected in the peak of the compressibility at the supercooling peak temperature. Our model indicates that the two liquids that are in equilibrium around −50 °C are cage structures and broken H-bonded pieces, 2HB.[7]

Second, CageWater predicts a liquid−liquid phase transition with a critical point. Figure 5a shows the temperature dependence of the average number of hydrogen bonds. At pressures above about 100 MPa, there is a sharp, nearly discontinuous change from 4 to 3.6 hydrogen bonds upon warming supercold water. At higher temperatures, above the liquid−liquid critical point, the average number of HBs changes more continuously. Figure 5b shows the corresponding changes in the chemical potential. The model predicts a first-order liquid −liquid pressure-driven phase transition at 3.6 hydrogen bonds per water molecule. The figures also show that for pressures above 1000 MPa the model no longer predicts a transition. At those extreme pressures even the coldest temperatures cannot stabilize the cages relative to more compact crunched-down structures.

Third, Figure 5c and 5d gives two views of the model's liquid−liquid phase transition and critical point: temperature vs density and pressure vs temperature. It compares the predictions of CageWater (black) and TIP4P/2005[82] (green). While both models show a 2-phase transition ending in a critical point, they disagree numerically. The critical point is given by TIP4P/2005 as (T, p) = (−80 °C, 174 MPa) and by CageWater as (−150 °C, 394 MPa). It is not clear whether this discrepancy is because of inaccuracies in CageWater in supercooled water or limitations, for example, in sampling, in the TIP simulations.

Another test of the CageWater model is its prediction of stretched water, i.e., at negative pressures. Figure 6 shows experiments on the TMD (temperatures of maximum density, measured by sound velocities) for pressures between −100 and 0 MPa[84] in comparison to simulations of the TIP4P/2005 model[85] and our CageWater modeling here.[86–89] While the models diverge from each other at the extremes, both models are consistent with the data over its range.

We note that our CageWater model has more parameters (11, Table S1) than TIP4P/2005 (8, Table S2), a standard in the field. This may account for its good prediction accuracy. However, we note that all of the parameters are physical and that the CageWater model contains simple approximations to physics that TIP4P leaves out, namely, a nonelectrostatic component to the angle dependence of H bonds and a correlation strength among H-bonded waters.

Author Manuscript Author Manuscript Author Manuscript Author Manuscript

CONCLUSIONS

We develop an analytical theory of water (CageWater) and apply it to explaining how the pVT properties of liquid water arise from water's hydrogen bonding and contacts. It predicts volumetrics and energetics more accurately than explicit simulation models yet is much faster to compute. Its simplicity and predictive power come from representing water using only three factors in the partition function, 2-body H bonds, 2-body contacts, and 12-body cooperative cages, rather than as a more extensive density expansion, for example. CageWater advances our understanding of water's structure−property relations in showing that (i) water's long-known 2-density behavior is encoded in relatively infrequent cages (ii) which melt out strongly with temperature and pressure and remarkably (iii) the balance of forces—particularly in the supercooled liquid—is not water's pairwise hydrogen bonds against van der Waals contacts but against the hydrogen bonds inside the cooperative cages. This understanding of water structure−property relations may aid in engineering filtration, osmosis, and desalination materials, in better solvation models for drugs and biomolecule actions, and for interpreting planetary geochemistry and hydrological cycles.

Supplementary Material

Refer to Web version on PubMed Central for supplementary material.

ACKNOWLEDGMENTS

We are grateful for support from the NIH (GM063592) and Slovenian Research Agency (P1 0103–0201, N1–0042). We thank Chris Fennell, Miha Luksic, Pablo Debenedetti, Teresa Head-Gordon, Thanos Panagiotopoulos, Tom Truskett, and Pradipta Bandyopadhyay for very helpful discussions.

REFERENCES

(1). Dill KA; Truskett TM; Vlachy V; Hribar-Lee B Annu. Rev. Biophys. Biomol. Struct 2005, 34, 173. [PubMed: 15869376]

(2). Rahman A; Stillinger FH J. Chem. Phys 1971, 55, 3336–3359.

(3). Berendsen HJC; Grigera JR; Straatsma TP J. Phys. Chem 1987, 91, 6269–6271.

(4). Abascal JLF; Vega CJ Chem. Phys 2005, 123, 234505.

(5). Jorgensen WL; Jenson CJ Comput. Chem 1998, 19, 1179.

(6). Molinero V; Moore EB J. Phys. Chem. B 2009, 113, 4008–l4016. [PubMed: 18956896]

(7). Gallo P; Amann-Winkel K; Angell CA; Anisimov MA; Caupin F; Chakravarty C; Lascaris E; Loerting T; Panagiotopoulos AZ; Russo J; Sellberg JA; Stanley HE; Tanaka H; Vega C; Xu L; Pettersson LG M. Chem. Rev 2016, 116, 7463.

(8). In Water, a Comprehensive Treatise; Franks F, Ed.; Plenum Press: New York, 1972–1980; Vols. 1−7.

(9). Eisenberg D; Kauzmann W The structure and properties of water; Oxford University Press: Oxford, 1969.

(10). Stillinger FH Science 1980, 209, 451. [PubMed: 17831355]

(11). Tanford C The hydrophobic effect: formation of micelles and biological membranes, 2nd ed.; Wiley: New York, 1980.

(12). Blokzijl W; Engberts JB Angew FN. Chem., Int. Ed. Engl 1993, 32, 1545.

(13). Robinson G; Zhu S-B; Singh S; Evans M Water in Biology, Chemistry and Physics: Experimental Overviews and Computational Methodologies; World Scientific: Singapore, 1996.

(14). Schmid R Monatsh. Chem 2001, 132, 1295.

Author Manuscript Author Manuscript Author Manuscript Author Manuscript

(15). Guillot BJ Mol. Liq 2002, 101, 219.
(16). Ben-Naim A Biophys. Chem 2003, 105, 183. [PubMed: 14499891]
(17). Pratt LR Annu. Rev. Phys. Chem 2002, 53, 409. [PubMed: 11972014]
(18). Jorgensen WL; Chandrasekhar J; Madura JD; Impey RW; Klein ML J. Chem. Phys 1983, 79, 926.
(19). Nezbeda IJ Mol. Liq 1997, 73–74, 317.
(20). Nezbeda I; Kolafa J; Kalyuzhnyi Yu. V. Mol. Phys 1989, 68, 143.
(21). Nezbeda I; Iglesias-Silva GA Mol. Phys 1990, 69, 767.
(22). Vega C; Abascal JLF; Conde MM; Aragones JL Faraday Discuss 2009, 141, 251. [PubMed: 19227361]
(23). Ben-Naim AJ Chem. Phys 1971, 54, 3682.
(24). Ben-Naim A Mol. Phys 1972, 24, 705.
(25). Truskett TM; Debenedetti PG; Sastry S; Torquato SJ Chem. Phys 1999, 111, 2647.
(26). Holten V; Bertrand CE; Anisimov MA; Sengers JV J. Chem. Phys 2012, 136, 094507. [PubMed: 22401452]
(27). Holten DT; Limmer V; Molinero V; Anisimov MA J. Chem. Phys 2013, 138, 174501. [PubMed: 23656138]
(28). Bertrand CE; Anisimov MA J. Phys. Chem. B 2011, 115, 14099. [PubMed: 21661753]
(29). Holten V; Anisimov MA Sci. Rep 2012, 2, 713. [PubMed: 23056905]
(30). Poole PH; Sciortino F; Grande T; Stanley HE; Angell CA Phys. Rev. Lett 1994, 73, 1632. [PubMed: 10056844]
(31). Roberts CJ; Debenedetti PG J. Chem. Phys 1996, 105, 658.
(32). Pretti M; Buzano C; De Stefanis EJ Chem. Phys 2009, 131, 224508.
(33). Tanaka HJ Chem. Phys 2000, 112, 799.
(34). Tanaka H Europhys. Lett 2000, 50, 340.
(35). Roentgen WC Ann. Phys 1892, 281, 91.
(36). Mishima O; Stanley HE Nature (London, U. K.) 1998, 396, 329.
(37). Beveridge DL; Mezei M; Mehrotra PK; Marchese FT; Ravishanker G; Vasu TR; Swaminathan S In Molecular Based Study of Fluids; Haile JM, Mansoori GA, Eds.; American Chemical Society: Washington, D.C., 1983; p 297.
(38). Beveridge DL; Mezei M; Mehrotra PK; Marchese FT; Ravishanker G; Vasu TR; Swaminathan S Adv. Chem. Ser 1983, 204, 297.
(39). Ben-Naim A Water and Aqueous Solutions, Introduction to a Molecular Theory; Plenum: New York, 1974.
(40). Clark GNI; Cappa CD; Smith JD; Saykally RJ; Head-Gordon T Mol. Phys 2010, 108, 1415–1433.
(41). Xu L; Buldyrev SV; Angell CA; Stanley HE Phys. Rev. E 2006, 74, 031108.
(42). Debenedetti PG Metastable Liquids, Concepts and Principles; Princeton University Press, 1996.
(43). Holten V; Palmer JC; Poole PH; Debenedetti PG; Anisimov MA J. Chem. Phys 2014, 140, 104502 Two-state thermodynamics of the ST2 model for supercooled water. . [PubMed: 24628177]
(44). Urbic T; Dill KA J. Chem. Phys 2010, 132, 224507. [PubMed: 20550408]
(45). Urbic T Phys. Rev. E 2012, 85, 061503.
(46). Urbic T Phys. Rev. E: Stat. Phys., Plasmas, Fluids, Relat. Interdiscip. Top 2016, 94, 042126.
(47). Truskett TM; Dill KA J. Chem. Phys 2002, 117, 5101.
(48). Truskett TM; Dill KA J. Phys. Chem. B 2002, 106, 11829.
(49). Jagla EA J. Chem. Phys 1999, 111, 8980.
(50). Dill KA; Bromberg S Molecular Driving Forces: Statistical Thermodynamics in Biology, Chemistry, Physics, and Nanoscience, 2nd ed.; Garland Science, 2010.
(51). Hare DE; Sorensen CM J. Chem. Phys 1990, 93, 6954–6960.
(52). Kalinichev AG; Bass JD J. Phys. Chem. A 1997, 101, 9720.

Author Manuscript Author Manuscript Author Manuscript Author Manuscript

(53). Gorbaty YE; Demianets YN Chem. Phys. Lett 1983, 100, 450.
(54). Nieto-Draghi C; Bonet Avalos J; Rousseau BJ Chem. Phys 2003, 118, 7954–7964.
(55). Wernet P; Nordlund D; Bergmann U; Cavalleri M; Odelius M; Ogasawara H; Naslund LA; Hirsch TK; Ojamae L; Glatzel P; Pettersson LGM; Nilsson A Science 2004, 304, 995–999. [PubMed: 15060287]
(56). Luck WA P. Discuss. Faraday Soc 1967, 43, 115.
(57). Suresh SJ; Naik VM J. Chem. Phys 2000, 113, 9727–9732.
(58). Haggis GH; Hasted JB; Buchanan TJ J. Chem. Phys 1952, 20, 1452–1465.
(59). Hoffmann MM; Conradi MS J. Am. Chem. Soc 1997, 119, 3811.
(60). Bondarenko GV; Gorbaty Yu. E. Mol. Phys 1991, 74, 639–647.
(61). Prada-Gracia D; Shevchuk R; Rao FJ Chem. Phys 2013, 139, 084501.
(62). Sellberg JA; Huang C; McQueen TA; Loh ND; Laksmono H; Schlesinger D; Sierra RG; Nordlund D; Hampton CY; Starodub D; DePonte DP; Beye M; Chen C; Martin AV; Barty A; Wikfeldt KT; Weiss TM; Caronna C; Feldkamp J; Skinner LB; Seibert MM; Messerschmidt M; Williams GJ; Boutet S; Pettersson LGM; Bogan MJ; Nilsson A Nature 2014, 510, 381. [PubMed: 24943953]
(63). Speedy RJ; Angell CA J. Chem. Phys 1976, 65, 851.
(64). Poole PH; Sciortino F; Essmann U; Stanley HE Nature 1992, 360, 324.
(65). Sciortino F; Geiger A; Stanley E Phys. Rev. Lett 1990, 65, 3452. [PubMed: 10042875]
(66). Limmer DT; Chandler DJ Chem. Phys 2011, 135, 134503.
(67). Smith JD; Cappa CD; Wilson KR; Cohen RC; Geissler PL; Saykally RJ Proc. Natl. Acad. Sci. U. S. A 2005, 102, 14171–14174. [PubMed: 16179387]
(68). Geissler PL J. Am. Chem. Soc 2005, 127, 14930–14935. [PubMed: 16231949]
(69). Sastry S; Debenedetti PG; Sciortino F; Stanley HE Phys. Rev. E: Stat. Phys., Plasmas, Fluids, Relat. Interdiscip. Top 1996, 53, 6144.
(70). Palmer JC; Haji-Akbari A; Singh RS; Martelli F; Car R; Panagiotopoulos AZ; Debenedetti PG J. Chem. Phys 2018, 148, 137101; J. Chem. Phys. 2018, 148, 137101. [PubMed: 29626877]
(71). Debenedetti PG J. Phys.: Condens. Matter 2003, 15, R1669.
(72). Palmer JC; Poole PH; Sciortino F; Debenedetti PG Chem. Rev 2018, 118, 9129–9151. [PubMed: 30152693]
(73). Xu Y; Petrik NG; Smith RS; Kay BD; Kimmel GA Proc. Natl. Acad. Sci. U. S. A 2016, 113, 14921–14925. [PubMed: 27956609]
(74). Palmer JC; Martelli F; Liu Y; Car R; Panagiotopoulos AZ; Debenedetti PG Nature 2014, 510, 385–388. [PubMed: 24943954]
(75). Pallares G; El Mekki Azouzi M; Gonzalez MA; Aragones JL; Abascal JL; Valeriani C; Caupin F Proc. Natl. Acad. Sci. U. S. A 2014, 111, 7936–7941. [PubMed: 24843177]
(76). Abascal JLF; Vega CJ Chem. Phys 2010, 133, 234502.
(77). Wikfeldt KT; Nilsson A; Pettersson GM Phys. Chem. Chem. Phys 2011, 13, 19918–19924. [PubMed: 21915406]
(78). Santra B; DiStasio RA Jr.; Martelli F; Car R Mol. Phys 2015, 113, 2829–2841.
(79). English NJ; Tse JS Phys. Rev. Lett 2011, 106, 037801. [PubMed: 21405300]
(80). Mallamace F; Corsaro C; Stanley HE Proc. Natl. Acad. Sci. U. S. A 2013, 110, 4899–4904. [PubMed: 23483053]
(81). Ni Y; Skinner JJ Chem. Phys 2016, 144, 214501.
(82). Singh RS; Biddle JW; Debenedetti PG; Anisimov MAJ. Chem. Phys 2016, 144, 144504. [PubMed: 27083735]
(83). Smallenburg F; Sciortino F Phys. Rev. Lett 2015, 115, 015701. [PubMed: 26182107]
(84). Holten V; Qiu C; Guillerm E; Wilke M; Rička J; Frenz M; Caupin FJ Phys. Chem. Lett 2017, 8, 5519–5522.
(85). González MA; Valeriani C; Caupin F; Abascal JL F. J. Chem. Phys 2016, 145, 054505.
(86). Luck WA P. J. Mol. Struct 1998, 448, 131.

Author Manuscript Author Manuscript Author Manuscript Author Manuscript

(87). Vega C; Abascal JLF; Nezbeda IJ Chem. Phys 2006, 125, 034503.
(88). Saul A; Wagner WJ Phys. Chem. Ref. Data 1989, 18, 1537.
(89). Wagner W; Saul A; Pruss AJ Phys. Chem. Ref. Data 1994, 23, 515.

Author Manuscript Author Manuscript Author Manuscript Author Manuscript

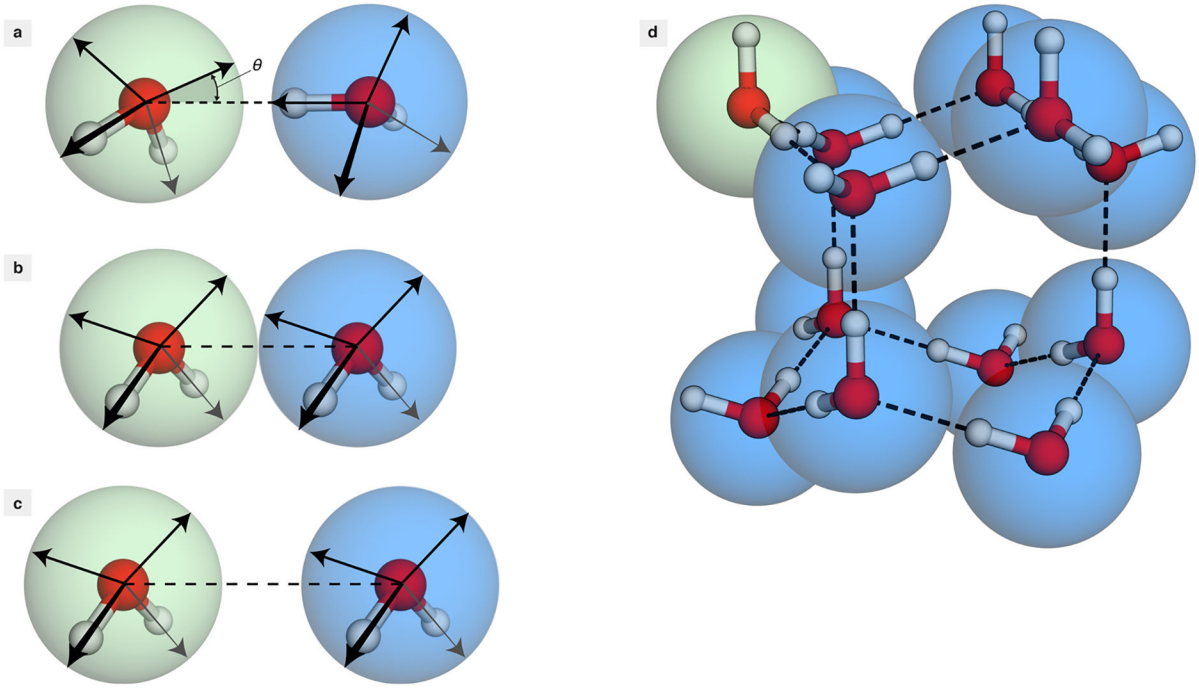

Figure 1.
Model states: (a) pairwise hydrogen bond (2HB); (b) pairwise contact, no hydrogen bond (c); (c) noninteracting (0); (d) cage structure (cage).

Author Manuscript Author Manuscript Author Manuscript Author Manuscript

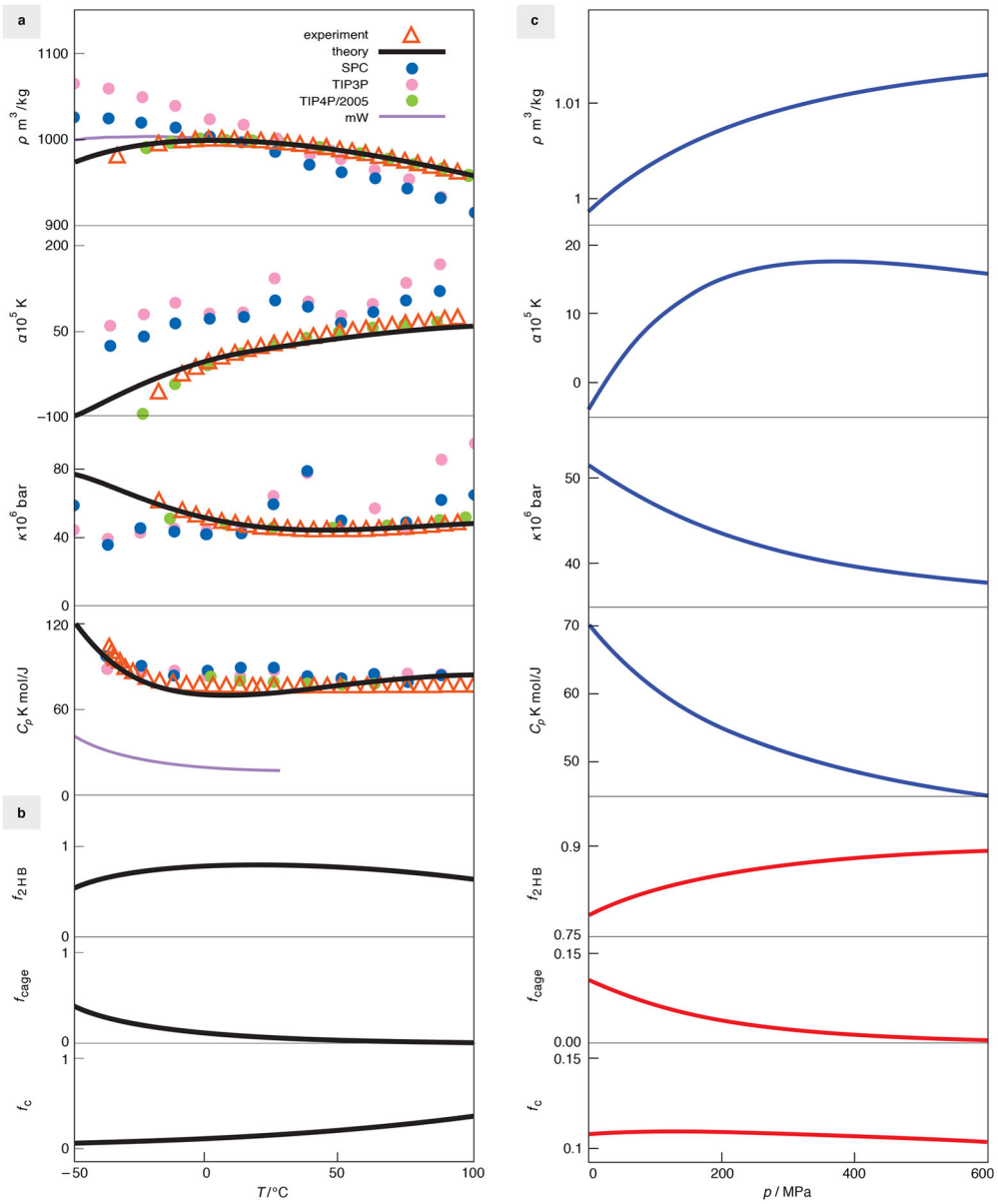

Figure 2.

Experimental liquid water properties vs model predictions and computer simulations. (a) Temperature dependence of liquid water's density, thermal expansion coefficient, isothermal compressibility, and heat capacity at 1 bar pressure. Experiments from ref 9. Computer simulations from refs 4 and 5, and mW model predictions from ref 6. (b) Molecular constituents of water at different temperatures: 2HB (pairwise hydrogen-bonded waters), cage (12-mer hexagons), and c (waters in contact but not hydrogen bonded). (c) Pressure dependences of the same properties and their constituents at a temperature of 273 K.

Author Manuscript Author Manuscript Author Manuscript Author Manuscript

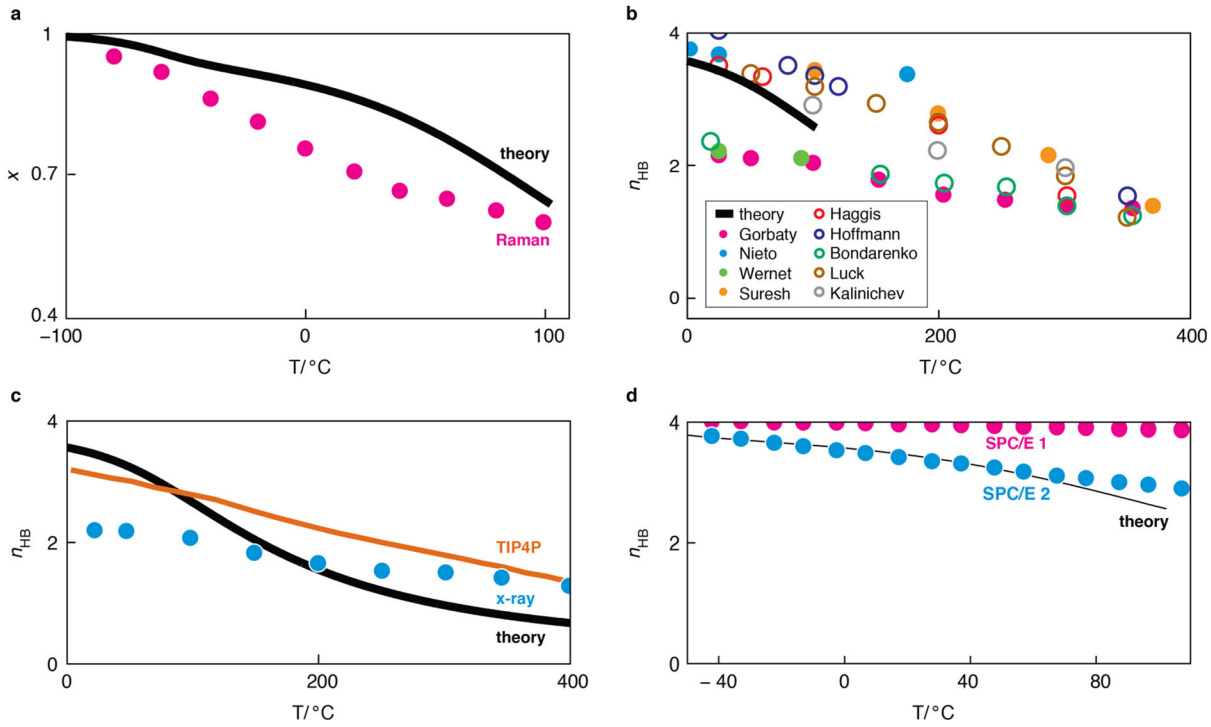

Figure 3.

Liquid water hydrogen bonding decreases with temperature: theory vs experiments. (a) Fraction of hydrogen bonds made in liquid water vs temperature. Data is Raman spectroscopy of the OH stretch region (2900−3800 cm^{-1}) by Hare and Sorensen.[51] (b) Number of hydrogen bonds per water (the theory line is plotted only up to water's boiling point).[52–60] (c) Number of hydrogen bonds per water, at high pressure (100 MPa): CageWater vs TIP4P simulation[52] vs X-ray diffraction.[53] (d) Computer simulations of SPC/E water shows the variance in interpretation that results from different definitions of what constitutes a hydrogen bond compared to our definition.[61]

Author Manuscript
Author Manuscript
Author Manuscript
Author Manuscript

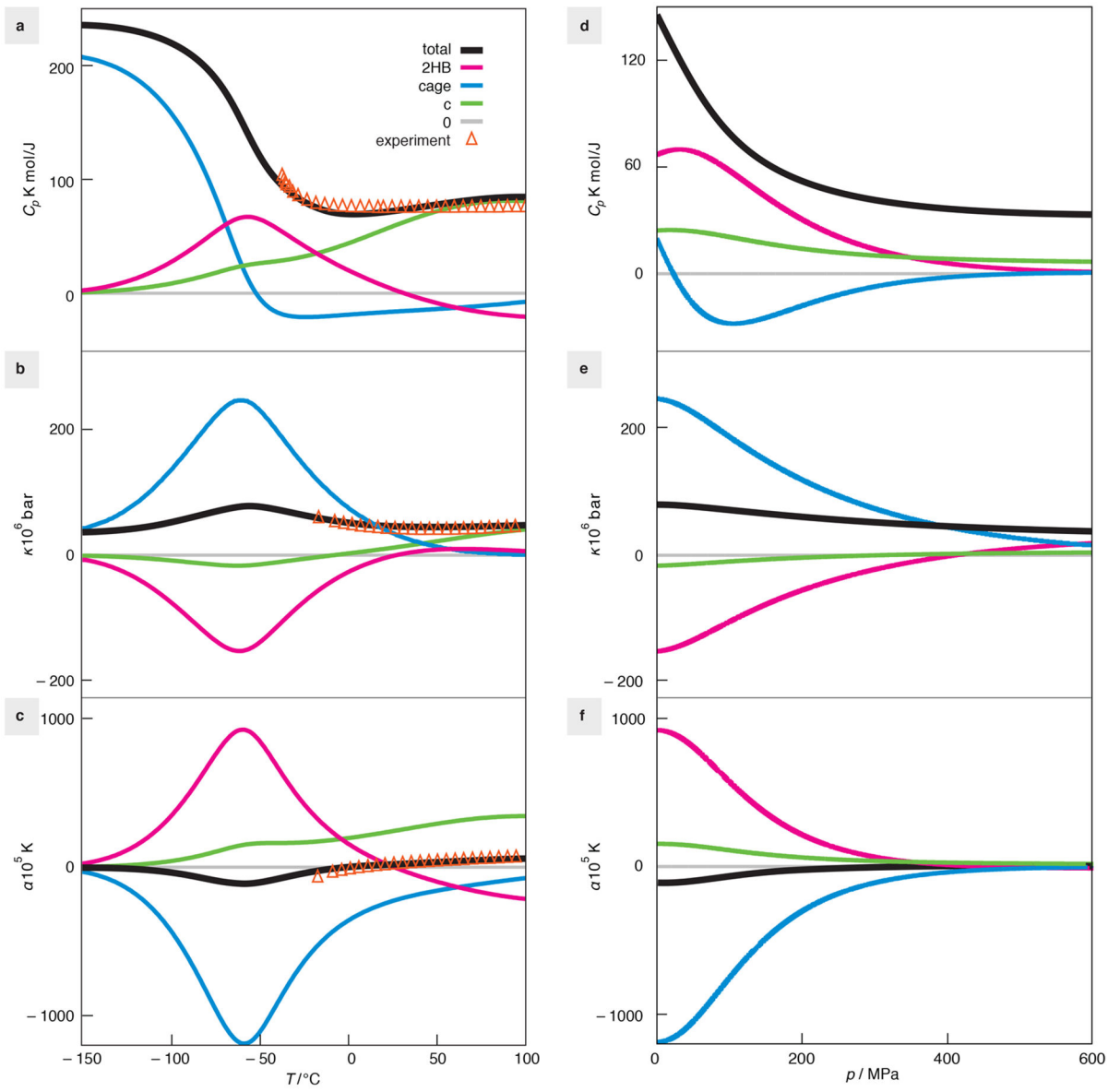

Figure 4.

Molecular components of supercooled water vary with temperature and pressure. Colored lines show the components 2HB (pairwise H bonded), cage (12-mer cages), c (waters in pairwise contact), 0 (waters separated and noncontacting). Black line is the sum of all components. Pressure dependence calculated at −35 °C. Temperature dependence at 0.1 MPa (1 atm). Most definitive features are the strong variations of the balance of molecular components with T and p and how strongly the caging behaviors are opposed by the pairwise hydrogen-bonded waters.

Author Manuscript Author Manuscript Author Manuscript Author Manuscript

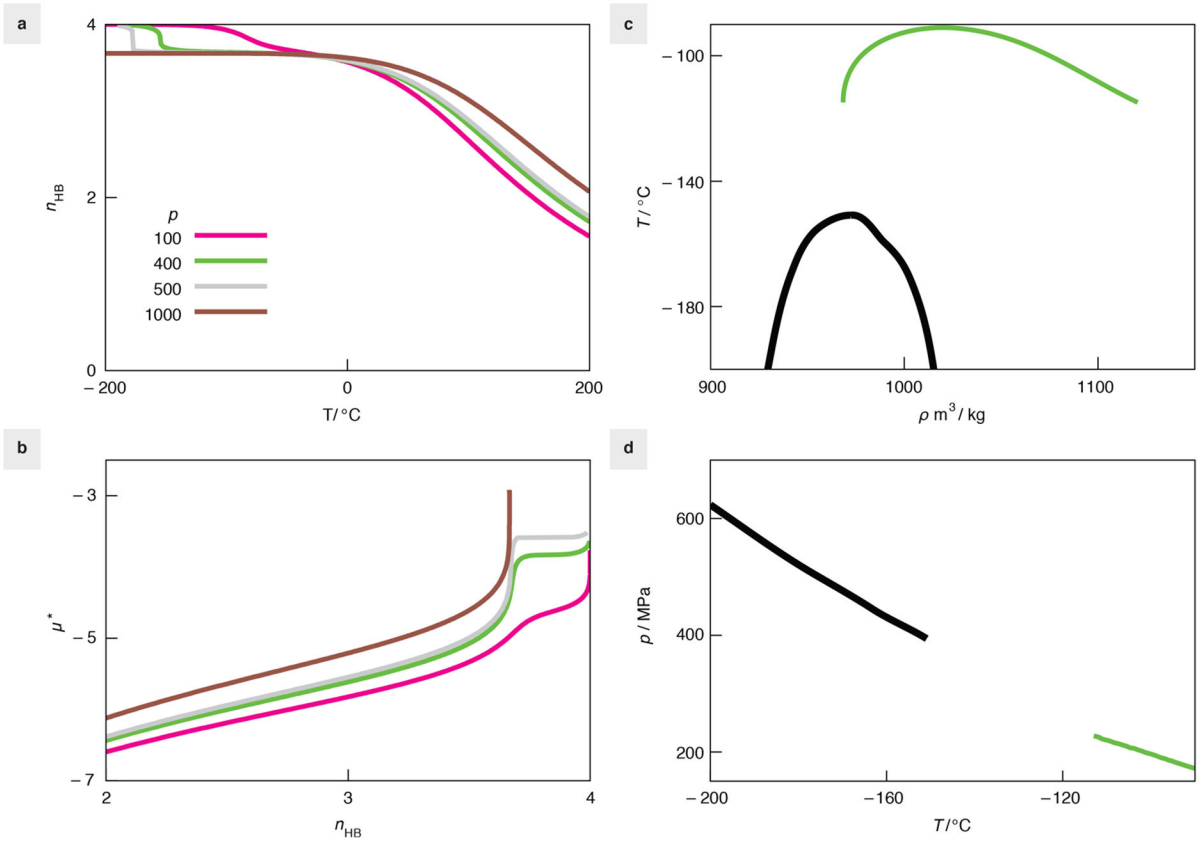

Figure 5.

Supercooled water has a phase transition with a critical point. (a) Number of hydrogen bonds per water undergoes a sharp change in cold water for a range of high pressures (pressure is reported in MPa). (b) Reduced excess chemical potential ($\mu^* = \mu/\epsilon_{HB}$) shows a first-order liquid−liquid pressure-driven phase transition at about 3.6 hydrogen bonds per water molecule. (c) Densities of coexistence of the two liquids from TIP4P/2005 simulations[82] (green solid line) and CageWater (black solid line). (d) Coexistence pressure as a function of temperature for TIP4P/2005 (green solid line) and CageWater (black solid line). Each curve in d terminates in a critical point at the right end. We are unaware of experimental data to test c and d.

Author Manuscript Author Manuscript Author Manuscript Author Manuscript

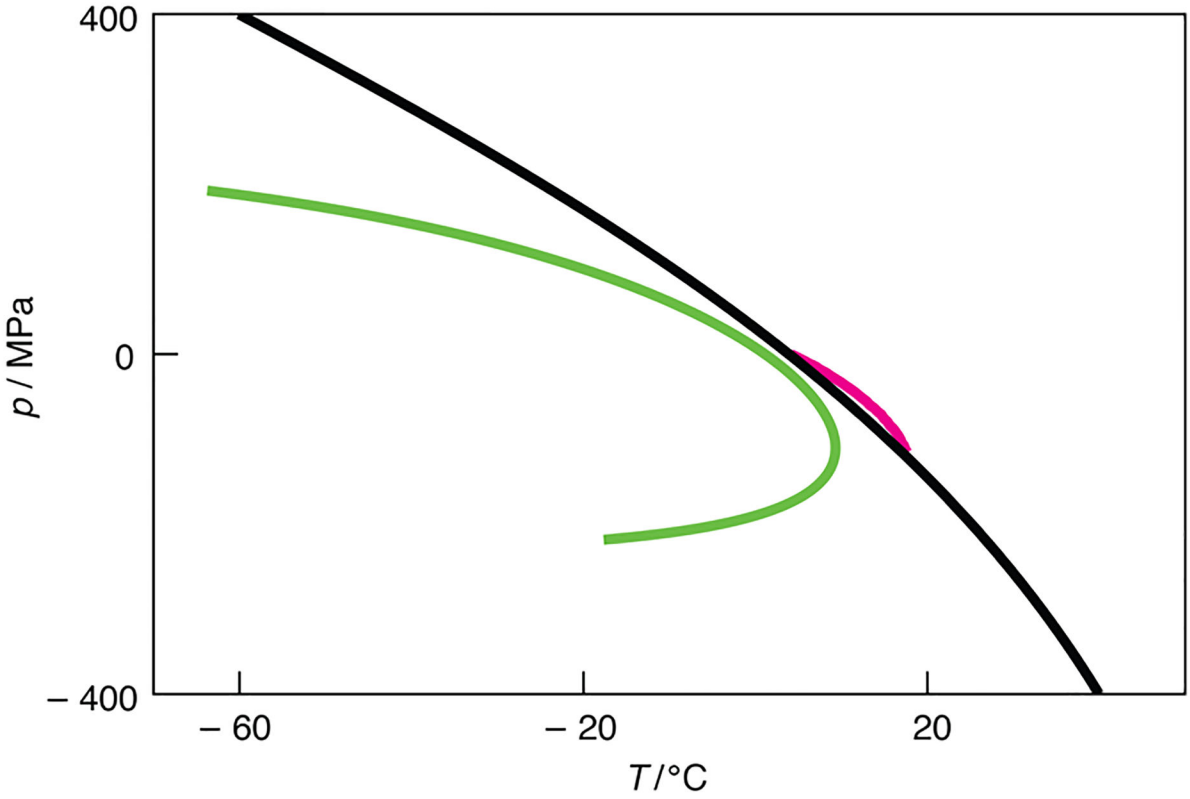

Figure 6.

pT behavior of stretched water (i.e., below 0 pressure). Lines of extrema in density from the sound velocity measurements (red solid curve)[84] are consistent with CageWater predictions (black solid line) as well as simulations of TIP4P/2005 (green line).[85]